

The Discovery and Characterization of a Proton-Gated Sodium Current in Rat Retinal Ganglion Cells

Sarah Lilley,¹ Paul LeTissier,² and Jon Robbins³

^{1,3}Neural Injury and Repair Group, Centre for Neuroscience Research, King's College London, Guy's Campus, London, SE1 1UL, United Kingdom, and

²Division of Neuroendocrinology, National Institute for Medical Research, The Ridgeway, Mill Hill, London, NW7 1AA, United Kingdom

The conduction of acid-evoked currents in central and sensory neurons is now primarily attributed to a family of proteins called acid-sensing ion channels (ASICs). In peripheral neurons, their physiological function has been linked to nociception, mechanoreception, and taste transduction; however, their role in the CNS remains unclear. This study describes the discovery of a proton-gated current in rat retinal ganglion cells termed $I_{\text{Na(H+)}}$, which also appears to be mediated by ASICs. RT-PCR confirmed the presence of ASIC mRNA (subunits 1a, 2a, 2b, 3, and 4) in the rat retina. Electrophysiological investigation showed that all retinal ganglion cells respond to rapid extracellular acidification with the activation of a transient Na^+ current, the size of which increases with increasing acidification between pH 6.5 and pH 3.0. $I_{\text{Na(H+)}}$ desensitizes completely in the continued presence of acid, its current–voltage relationship is linear and its reversal potential shifts with E_{Na^+} . $I_{\text{Na(H+)}}$ is reversibly inhibited by amiloride (IC_{50} , 188 μM) but is resistant to block by TTX (0.5 μM), Cd^{2+} (100 μM), procaine (10 mM), and is not activated by capsaicin (0.5 μM). $I_{\text{Na(H+)}}$ is not potentiated by Zn^{2+} (300 μM) or Phe-Met-Arg-Phe-amide (50 μM) but is inhibited by neuropeptide-FF (50 μM). Acute application of pH 6.5 to retinal ganglion cells causes sustained depolarization and repetitive firing similar to the trains of action potentials normally associated with current injection into these cells. The presence of a proton-gated current in the neural retina suggests that ASICs may have a more diverse role in the CNS.

Key words: acid-sensing ion channel; retinal ganglion cell; sodium channel; proton-gated current; retina; pH

Introduction

Proton-gated currents are emerging as a common feature of mammalian central and sensory neurons. In peripheral tissues, where ischemia-induced acidosis can measure several pH units, these currents have been implicated in nociception (Reeh and Steen, 1996; Benson and Sutherland, 2001), in addition to the physiological processes of mechanoreception (Price et al., 2000) and taste transduction (Gilbertson et al., 1993). The functional significance of currents gated by protons in the brain is less obvious, because the brain is well protected from such large pH fluxes by the carbonic anhydrase-catalyzed $\text{CO}_2/\text{HCO}_3^-$ buffering system (Chesler, 1990). Nevertheless, neurons from various regions of the brain and spinal cord respond to rapid extracellular acidification by conducting non-voltage-dependent cation currents carried predominantly, if not exclusively, by Na^+ . These currents are inhibited by the diuretic amiloride but are insensitive to TTX (Ueno et al., 1992; Baumann et al., 1996; Li et al., 1997; Varming, 1999).

In the CNS, there is strong evidence linking these proton-gated currents to a subgroup of the degenerin (DEG)–epithelial

Na^+ channel (ENaC) superfamily known as acid-sensing ion channels (ASICs). This evidence includes the absence of proton-gated currents in the hippocampal neurons of ASIC 1a knock-out mice (Wemmie et al., 2002), the distribution of ASIC-encoding mRNA throughout the CNS, and extensively studied parallels between neuronal proton-gated currents and those recorded from transfected cells expressing ASIC channel protein (Lingueglia et al., 1997; Waldmann et al., 1997; de Weille et al., 1998; Bassler et al., 2001). ASICs share their protein structure, amiloride sensitivity, and conduction of Na^+ -selective currents with the rest of the ENaC superfamily (de la Rosa et al., 2000) but are the only family members to be activated by protons. From ASIC genes cloned to date, seven subunit products (including splice variants) have been identified: ASIC1a, 1b, 1b2, 2a, 2b, 3, and 4; all but ASIC1b and 1b2 have been found in central neurons. By homomultimeric or heteromultimeric association of their subunits, ASICs conduct currents with a range of subtle variations in current characteristics. These reflect regional variations seen in “native” proton-gated currents recorded from both central and peripheral nervous tissue. With the recent synaptic localization of some ASICs (Wemmie et al., 2002), highly localized pH changes accompanying neurotransmitter release from vesicles may be large enough to briefly overcome interstitial buffering and activate these channels, perhaps giving ASICs a role in normal neurotransmission.

The retina is a functionally distinct region of central neurons known to contain ENaCs (Matsuo, 1998; Golestaneh et al., 2000) but has been demonstrated only recently to contain ASICs

Received July 4, 2003; revised Oct. 28, 2003; accepted Nov. 12, 2003.

This work was funded by the Wellcome Trust and University of London Central Fund. We gratefully acknowledge Drs. Melanie Clements and Pam Houston for their technical assistance.

Correspondence should be addressed to Dr. Jon Robbins, Neural Injury and Repair Group, Centre for Neuroscience Research, King's College London, Guy's Campus, London, SE1 1UL, UK. E-mail: jon.robbins@kcl.ac.uk.

S. Lilley's present address: Division of Neurophysiology, National Institute for Medical Research, The Ridgeway, Mill Hill, London, NW7 1AA, UK.

DOI:10.1523/JNEUROSCI.3191-03.2004

Copyright © 2004 Society for Neuroscience 0270-6474/04/241013-10\$15.00/0

Table 1. Nomenclature, cloning, and RT-PCR primer sequence details of the six rat ASIC subunits examined for their presence in the retina

Subunit	Accession number	Alternative published names	Forward (f) and reverse (r) primer sequences (listed 3' to 5')	Annealing temperature (°C)	Product size (nucleotides)
ASIC1a	U94403 (rat)	BNaC2, ASIC	f: GCTTTAGCCAAGTCTCCAAG r: AGTCAAAGAGTTCAGCACC	58.0	1064
ASIC1b	AJ006519 (rat)	ASIC- β	f: CTCTATTGTTCTACTGTGG r: CTTCTGGCACTTCCACGTC	50.5	905
ASIC2a	NM_012892 (rat)	BNaC1, MDEG, MDEG1	f: GCTCTACTGCAAGTCAAGG r: ACACCTCCTGTGCTGCTCAG	58.0	522
ASIC2b	Y14635 (rat)	MDEG2	f: ATATGCTGCTCTCTGCAAG r: ACACCTCCTGTGCTGCTCAG	58.0	529
ASIC3	AF013598 (rat)	DRASIC	f: TGACATGGCACAACCTACG r: TCATTGACAGCCCACTTC	61.0	568
ASIC4	AJ242554 (rat) (truncated protein in pituitary: AJ271642)	SPASIC	f: TATAGTGTGCTGCTGCGG r: TGTAGGTCCTATTGCGGTTG	58.0	288

(Brockway et al., 2002; Maubaret et al., 2002). Retinal ganglion cells (RGCs) are an interesting potential location of these channels as they undergo constant, rapid stimulation in both light and darkness while collating all visual input from the retina. They exhibit a high level of metabolic activity, which has been shown to cause transient interstitial acidification around the optic nerve during normal neurotransmission (Davis et al., 1987). The present study examines the rat retina for evidence of ASIC channels and characterizes the response of RGCs to extracellular acidification. A brief report of some of this data has been published (Lilley and Robbins, 2001).

Materials and Methods

All animal procedures were approved by the university ethics committee and adhere to United Kingdom Home Office regulations.

Reverse transcriptase-PCR. Hooded Lister rats [postnatal d (P) 18; either gender] were killed by decapitation. The eyes were removed, and the retina was extracted. From the same animals, brain tissue (divided in a nonregion-specific manner) and the dorsal root ganglia (DRGs) were used to provide positive PCR controls. RNA was extracted using a modified version of the method described by Chomczynski and Sacchi (1987) involving the use of Trizol (1 ml per 100 mg of tissue; Invitrogen, Paisley, UK). After extraction, the RNA was resuspended in RNase-free water (Sigma, Poole, UK), and sample content-purity was assessed by spectrophotometry. All reagents for cDNA generation were supplied by Promega (Hawthorne, Australia). Samples of nucleotide solution (20 μ l) containing 5 μ g of extracted RNA, 1 pmol oligo-dT primers, and RNase-free water were denatured at 70°C for 5 min. These were immediately cooled on ice before the addition of 10 nmol of deoxy-NTP (dNTP) substrate [equimolar dATP, dGTP, dCTP, and deoxythymidine triphosphate (dTTP)], 5 \times Moloney murine leukemia virus (M-MLV) reverse transcriptase (RT) reaction buffer, and 0.5 μ l of RNasin. After 5 min at room temperature, 1 μ l of M-MLV RT (200 U/ μ l) was added, and the sample was incubated at 42°C for 1 hr. Repeating the above process with the omission of the reverse transcriptase produced negative control samples for subsequent PCR reactions. PCR reactions were performed in volumes of 50 μ l containing PCR buffer, including 15 mM MgCl₂ (Roche Products, Hertfordshire, UK), 10 nmol of dNTP substrate (comprising equimolar dATP, dGTP, dCTP, and dTTP), 10 nmol each of forward and reverse primers (Sigma; Genosys, The Woodlands, TX) (see Table 1 for details), 0.5 μ l of a 16:1 (unit:unit) mix of *Taq* polymerase and Pfu (Roche Products), DNase- and RNase-free water (Sigma), and 1 μ l of either cDNA (RT+ reaction) or negative control (RT-) generated in the previous step. PCR was performed in 34 cycles of denaturation (94°C for 30 sec), annealing (see Table 1 for subunit-specific temperatures), and extension (72°C for 2 min). Products were viewed by 1.2% agarose gel electrophoresis.

Cell culture and RGC identification. RGCs were cultured as described by Robbins et al. (2003). Retinas from P2–P20 Hooded Lister rats were subjected to digestion by papain and gentle trituration, and the cell sus-

pension was centrifuged through a gradient mixture. Cells were resuspended by additional trituration to ensure good separation of the cells in culture. Mixed retinal cultures were plated onto poly-L-lysine-coated glass coverslips and maintained in modified DMEM–HBSS (Invitrogen) at 37°C and 5% CO₂ for 1–10 d before experimentation. RGCs were identified routinely from other cell types on the basis of soma diameter (>12 μ m), which was based on correlation with immunocytochemical staining (Thy1.1; Chemicon, Temecula, CA; FITC-IgC; Boehringer Mannheim, Mannheim, Germany) and patterns of electrical activity recorded using whole-cell current clamp (Lilley, 2001; Robbins et al., 2003).

Electrophysiology. Whole-cell membrane currents were recorded via a single electrode using the patch-clamp technique. All voltage-clamp recordings were taken from cells cultured for 1–2 d only to limit axonal development and thereby minimize space-clamp errors. Cells were bathed in solution containing (in mM): 140 NaCl, 5 KCl, 2.5 CaCl₂, 1 MgCl₂, 10 glucose, and 10 HEPES, pH adjusted to 7.33 using NaOH. In ion substitution experiments, NaCl was sequentially reduced from 140 to 45 to 14 mM and replaced with equimolar TEA-Cl, and the pH was adjusted using KOH. For Ca²⁺-free recordings, CaCl₂ was omitted, 1 mM EGTA was added, and MgCl₂ increased to 5 mM. Extracellular solution for all voltage-clamp recordings contained 0.5 μ M TTX (Tocris Cookson, Bristol, UK). Polished borosilicate glass pipettes (6–12 M Ω) were filled with the following (in mM): 110 Cs⁺ acetate, 20 CsCl, 20 NaCl, 10 HEPES, 3 EGTA, 3 MgCl₂, and 1 CaCl₂, pH adjusted to 7.33 with CsOH. For acute application of acid or other ligands to an individual cell, membrane voltage of the target cell was maintained at –80 mV. Rapid application was achieved using either single- or triple-barreled pipettes connected to a NeuroPhore BH-2 pressure ejection system (Digitimer, Hertfordshire, UK) or by U-tube perfusion as stated in Results. Where current–voltage relationships have been measured, pressure-pulse applications were combined with 15 mV depolarizations in cell-holding voltage over the range of –80 to 55 mV (each voltage being held for 40 sec before pressure pulses were applied to inactivate transient Ca²⁺ currents). Pressure-pulse triggering, voltage protocol application, and all data acquisition (sampled at 2 kHz) were achieved using pClamp6 via a Digidata 1200 interface (Axon Instruments, Foster City, CA). Cell responses were amplified using an Axopatch 1C and CyberAmp (Axon Instruments) with low-pass filtering at 600 Hz.

Figures comprising voltage-clamp data from multiple cells are plotted in terms of current density (pA/pF): a measure of current per unit area of cell membrane in which area is directly proportional to capacitance. Capacitance measurements for each cell were derived by recording uncompensated capacitance artifacts evoked by a short 20 mV hyperpolarizing step from which only the “fast pipette” component had been removed by compensation. The decay phase of these artifacts was fitted with an exponential curve, the time constant from which was divided by the series resistance measured for the cell to give an approximation of cell capacitance. All voltage-clamp recordings were then made with 80% series resistance compensation added via the amplifier, unless otherwise stated. Adjustment of reversal potentials to allow for ionic activity was

done with appropriate ion activity coefficients as listed by Robinson and Stokes (1959). For example, $140 \text{ mM NaCl} \times 0.778 = 108.9 \text{ mM free Na}^+$ ions at 25°C .

Current-clamp recordings were made from cells grown in culture from 3–10 d, which had begun to develop axonal processes. Standard extracellular solution was used with the omission of TTX. Intracellular solution comprised the following (in mM): 120 K^+ acetate, 20 KCl, 10 HEPES, 3 EGTA, 3 MgCl_2 , and 1 CaCl_2 , adjusted to pH 7.33 with KOH.

Test pH solution consisted of extracellular solution that was appropriate to the experiment acidified to the required pH using HCl. The pH of these acidified solutions was checked both before and after all experiments, because some acidity levels were beyond the normal range of the buffer (HEPES). However, pH was found to be stable throughout, so no buffering modifications were made. We were unable to use acid solutions stronger than pH 3.0, because this disrupted the seal between recording pipette and the cell membrane, hence the pH activation curve has not been “normalized” to a maximum value. Neuropeptide-FF (N-FF) and Phe-Met-Arg-Phe-amide (FMRFamide) were supplied by Peninsular (St. Helen’s, UK). Amiloride, capsaicin, and all other reagents were from Sigma.

Intracellular Ca^{2+} measurement. Procedures were similar to that described by Hayat et al. (2003). Briefly, mixed retinal cells cultured for 2–5 d were loaded with $5 \mu\text{M}$ 1-[2-amino-5-(6-carboxyindol-2-yl)phenoxy]-2-(2'-amino-5'-methylphenoxy)ethane-N,N,N',N'-tetraacetic acid pentaacetoxymethyl ester (INDO-1/AM; Calbiochem, Nottingham, UK) in dimethyl sulfoxide (DMSO; Sigma) for 1 hr at 37°C in the dark. The cultures were viewed using a Nikon Diaphot microscope and 330–380 nm excitation from a xenon light source. Fluorescent emission from the cells was measured via photomultiplier tubes at both 405 and 488 nm, amplified using a purpose-built ratio amplifier (T. Dyett, University College London, London, UK) and data acquired on a personal computer running pClamp6 software (Axon Instruments). Calcium calibration was performed as described by Hayat et al. (2003), in which $[\text{Ca}^{2+}]_i$ (in nM) = $722 (R - 0.28/3.94 - R)$, where R is emission ratio.

All results are given as mean \pm SEM. Curve fitting was performed using the equation $y = [A_1 - A_2/1 + (x/x_0)^p] + A_2$, where A_1 is minimum, A_2 is maximum, p is slope, and x_0 is midpoint location.

Results

Presence of ASIC-encoding mRNA in the retina

The presence of ASIC-encoding mRNA in the rat retina was confirmed using RT-PCR (Fig. 1). Positive control reactions were performed using cDNA generated from rat brain (ASIC subunits 1a, 2a, 2b, 4) and DRGs (ASIC 1b and 3) from which primer-annealing temperatures were deduced. When these experiments were repeated alongside rat retinal cDNA, the primers for subunits 1a, 2a, 2b, and 4 produced clear positive results, and a faint positive result was seen with the primers for ASIC 3. Consistent with data from other CNS regions, no evidence of the ASIC 1b subunit was found in the retina using this method.

Relationship between extracellular pH and $I_{\text{Na}(\text{H}^+)}$ activation

Initial observations of the RGC proton-gated current ($I_{\text{Na}(\text{H}^+)}$) were made by the pressure ejection of acidified extracellular solution, pH 4.5, directly onto individual cells. In every cell tested ($n = 79$), this evoked a rapid inward current. In 30 of these cells held at -80 mV , the peak inward current was $1056 \pm 72 \text{ pA}$. These currents peaked within 200–450 msec of the start of the pressure pulse. Despite desensitizing fully in the continued presence of the acid, currents could be re-evoked, with no reduction in current amplitude, after 40 sec perfusion with control, pH 7.33, extracellular solution. Examples of $I_{\text{Na}(\text{H}^+)}$ evoked over a range of membrane potentials from -80 to $+40 \text{ mV}$ are shown in Figure 2A.

$I_{\text{Na}(\text{H}^+)}$ in rat RGCs was evoked by rapid (msec) acidification only. Decreasing extracellular pH via the chamber perfusion sys-

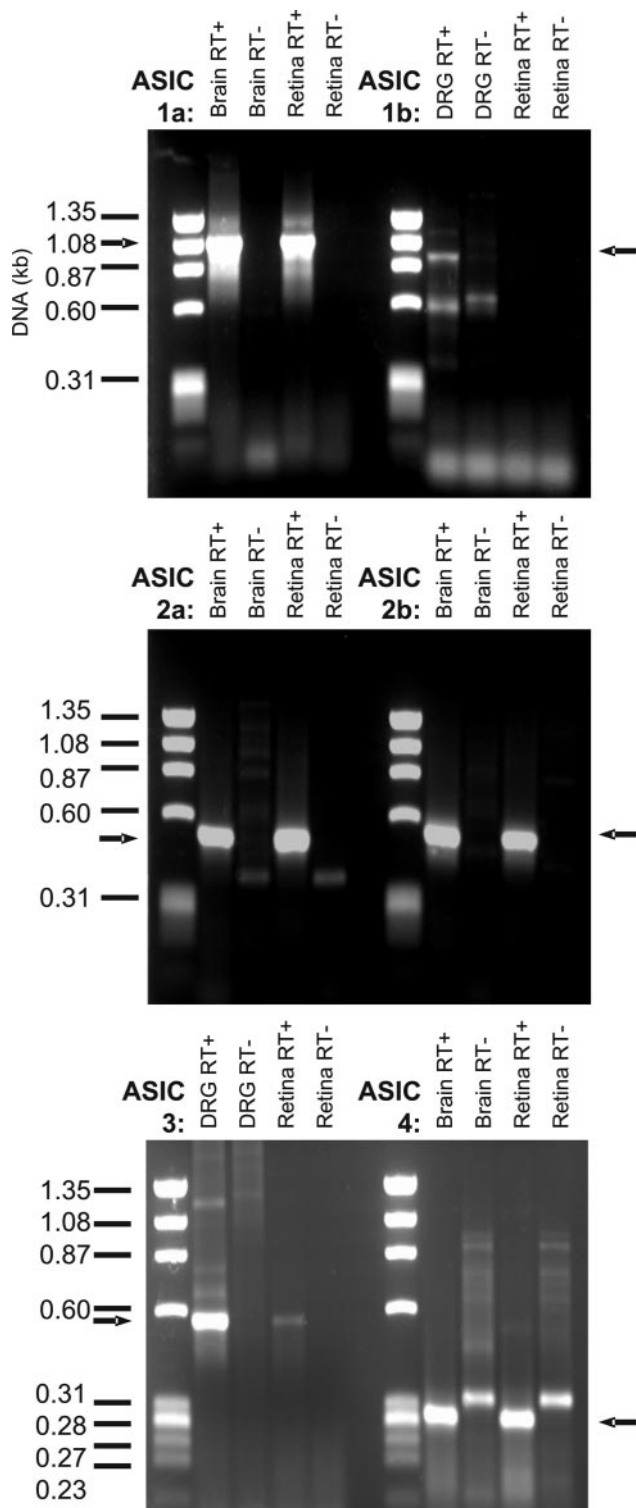


Figure 1. Evidence for the presence of ASIC-encoding mRNA in the rat retina. Whole retinal RNA was subject to RT-PCR using primers designed to detect the first six ASIC subunits cloned to date. Positive controls were performed using rat brain or DRG cDNA as appropriate. All RT-PCR experiments were repeated with the omission of reverse transcriptase to provide negative controls containing only genomic DNA rather than cDNA. Arrows indicate size of bands expected in RT+ samples.

tem over several seconds did not appear to evoke a depolarizing current, and there was no apparent overall change in membrane resistance with slow acidification.

The relationship between extracellular pH and RGC response

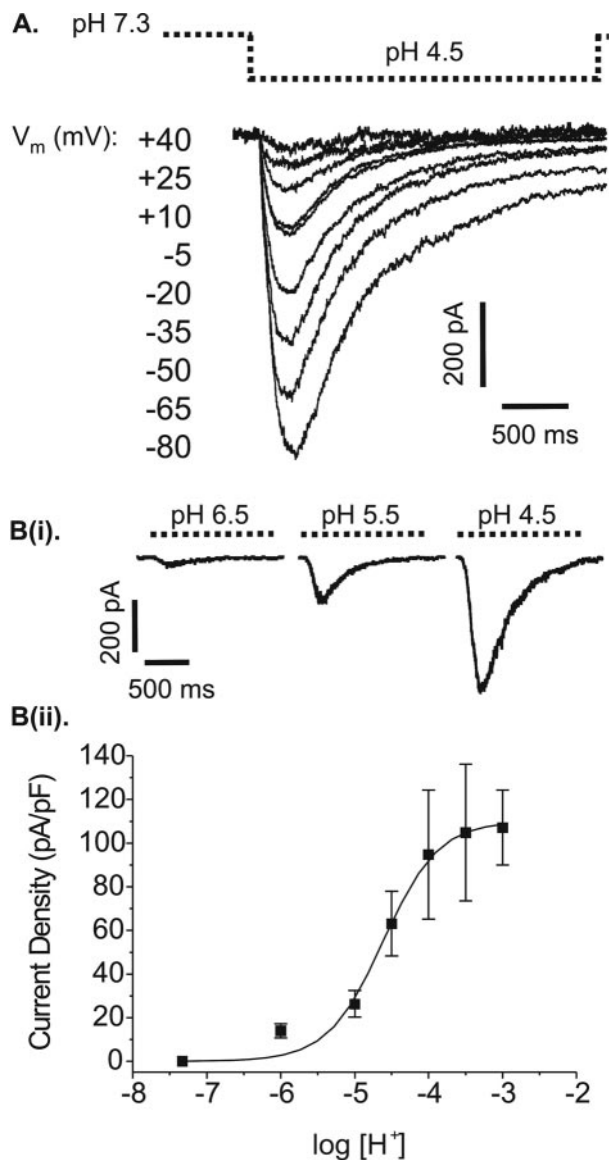


Figure 2. *A*, Example of pH 4.5-evoked currents in a single rat retinal ganglion cell at different membrane potentials. Cells were voltage clamped at the membrane potentials indicated in the figure. These membrane voltages were held for 40 sec before a 2 sec pressure pulse of acidified extracellular solution (pH 4.5) was applied to ensure any voltage-gated conductances were inactivated (dashed line indicates acid application). *Bi*, Currents evoked by different levels of extracellular acidification while cells were voltage-clamped at -80 mV (application by U-tube). *Bii*, Relationship between level of extracellular acidification and current activation in retinal ganglion cells. The pH-response graph, expressed in terms of current density, shows mean (\pm SEM) results for nonconsecutively administered pH test pulses recorded as in *Bi*. Each data point represents the mean current-density value for 7–13 cells at the given pH level. Test pulses of acid were administered in a randomized block design. Logistic fit: slope, 1.38; EC_{50} , pH 4.52.

was quantified using the U-tube system to attain an absolute, rather than relative, pH change across the surface of the target cell. Test solutions of pH 6.0, 5.0, 4.5, 4.0, 3.5, or 3.0 were applied in 3 sec pulses to each cell and repeated at 1 min intervals between which the cell was perfused with pH 7.33 solution. The mean current density for 7–13 cells at each given pH level is shown in Figure 2 *Bii* with individual examples in Figure 2 *Bi*. Peak inward current clearly increases with increasing acidity. The threshold for activation is pH 6.5, and current density approaches a maximum at pH 3.0. Half-maximal activation occurs at pH 4.5, which

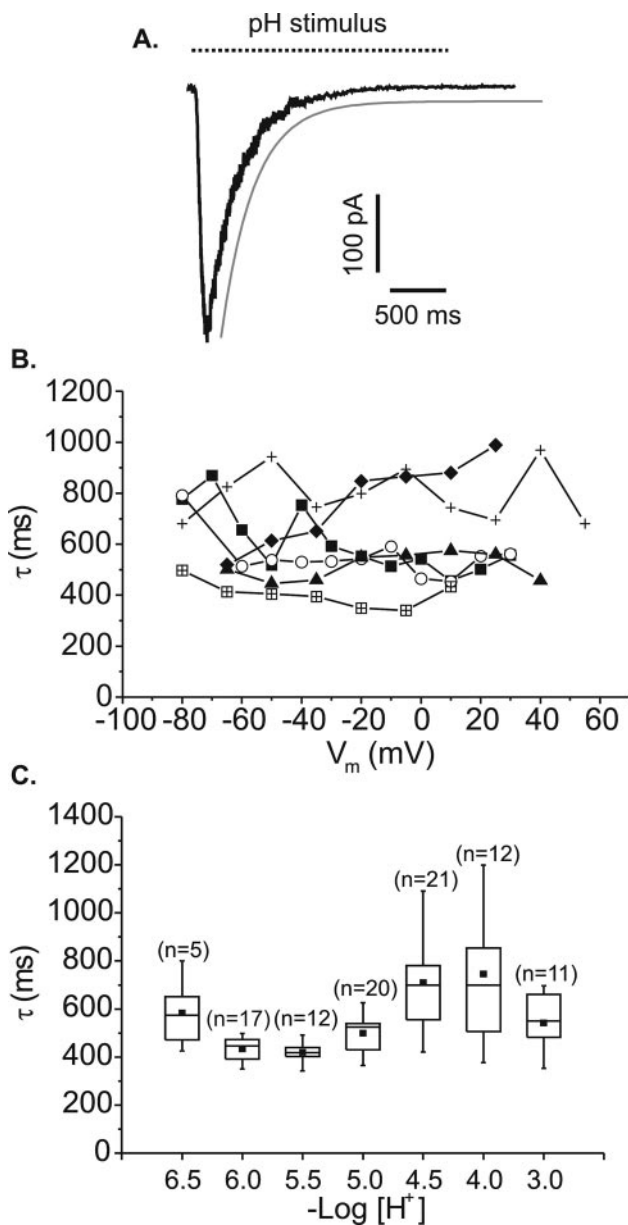


Figure 3. Current desensitization in the continued presence of acid. *A*, All time constants were derived from single exponential decay curves fitted as shown by the gray line. Dashed line represents 2.25 sec acidification by pressure pulse or 3 sec acidification by U-tube. *B*, Variation in the time constant of pH 4.5-evoked currents recorded from six rat retinal ganglion cells (linked symbols represent individual cells) while the cells were voltage clamped over a range of membrane potentials. Acid was applied by pressure-pulse ejection. *C*, Variation in the time constant of currents evoked by different strengths of acid recorded while cells were voltage clamped at a constant -80 mV (acid was applied by U-tube).

is used at the test pH for the majority of the following experiments.

Relationship between current desensitization, membrane voltage, and extracellular pH

Figure 3 shows the relationship between the time course of current desensitization in the continued presence of acid. The rate of desensitization and membrane voltage was examined using pressure pulses of pH 4.5 solution over a range of membrane voltages. An exponential curve was fitted to the decay phase of each evoked current from just after the current peak to the point corresponding to the end of the acid test pulse, as shown in Figure 3*A*. The

time constants (τ) of the exponential fits for six cells are plotted against membrane holding voltage in Figure 3B. All time constants were found to lie within the range of 300–1000 msec. For each cell, fluctuations can be seen across the potential range, but there is no obvious trend in the relationship between τ and membrane voltage. There was no evidence of a sustained component within the whole-cell current. All currents desensitized fully, although occasionally larger currents recorded at the more negative membrane potentials required longer than 2.25 sec to return to baseline.

To examine the relationship between rate of current desensitization and the strength of acid applied, test pulses of acid were applied by U-tube at a membrane holding voltage of -80 mV. Test solutions were administered in random order at 1 min intervals from a control pH of 7.33. In Figure 3C, the resultant time constants were pooled and plotted against $-\log[H^+]$. Again, there is variation across the pH range, but all mean values lie in the 400–700 msec range, and there is no obvious trend in the relationship between pH level and time course of current desensitization.

Sodium is the charge-carrying ion of $I_{Na(H^+)}$

The current–voltage relationship of the pH 4.5-evoked current in retinal ganglion cells is shown in Figure 4A. Because of its very positive reversal potential (65.1 ± 16.9 mV; $n = 9$) and in anticipation of the similarity between this and other transient neuronal proton-gated currents, Na^+ was investigated as a possible charge-carrying ion by measuring current–voltage relationships in different concentrations of extracellular Na^+ . Control I – V relationships were recorded in 140 mM $[Na^+]_o$ (Fig. 4A*i*); extracellular Na^+ concentration was then reduced to 45 mM (Fig. 4A*ii*) or 14 mM (Fig. 4A*iii*) by substitution of $[Na^+]_o$ with equimolar TEA-Cl. Accordingly, pH 4.5 test solutions were based on the corresponding extracellular solution. Although the larger non-permeant TEA⁺ ions introduced a degree of outward rectification, outward currents were recorded at membrane potentials positive to 34.7 ± 3.9 mV in 45 mM $[Na^+]_o$ and 6.9 ± 0.7 mV in 14 mM $[Na^+]_o$ ($n = 5$ in both cases). These reversal potentials have been adjusted for ionic activity and plotted along with a slope representing the theoretical relationship between $[Na^+]_o$ and E_{Na} for a pure Na^+ current derived using the Nernst equation in Figure 4B. The slope (58 mV/log fold $\Delta[Na^+]_o$) and the experimental data coincide completely, indicating that the RGC proton-gated current is carried by Na^+ .

Ca^{2+} microfluorimetry was used to confirm that no Ca^{2+} entered the cell through active proton-gated ion channels. Other research groups have previously noted that although the transient element of most neuronal responses to rapid extracellular acidification is conducted via Na^+ ions, a degree of Ca^{2+} conduction may be sustained by these channels (Kovalchuk et al., 1990). Figure 5, A and B, shows the $[Ca]_i$ measurements from a single retinal ganglion cell that has been loaded with the calcium fluorophore INDO-1/AM. Figure 5A shows a comparison of Ca^{2+} rises evoked in response to 10 sec pulses of either 100 μ M nicotine or pH 4.5 extracellular solution in the presence and absence of the voltage-gated Ca^{2+} channel blocker Cd^{2+} . This cell, like 23 of 43 others observed, showed an increase in intracellular Ca^{2+} in response to protons (49.8 ± 6.7 nM), which was blocked in the presence of Cd^{2+} . In contrast, responses to nicotine, which admits Ca^{2+} ions directly through nACh receptor-linked channels, remained unaffected in the same cells. This suggests that any $[Ca^{2+}]_i$ rise seen in RGCs in response to extracellular acidification is attributable to the secondary activation of voltage-gated

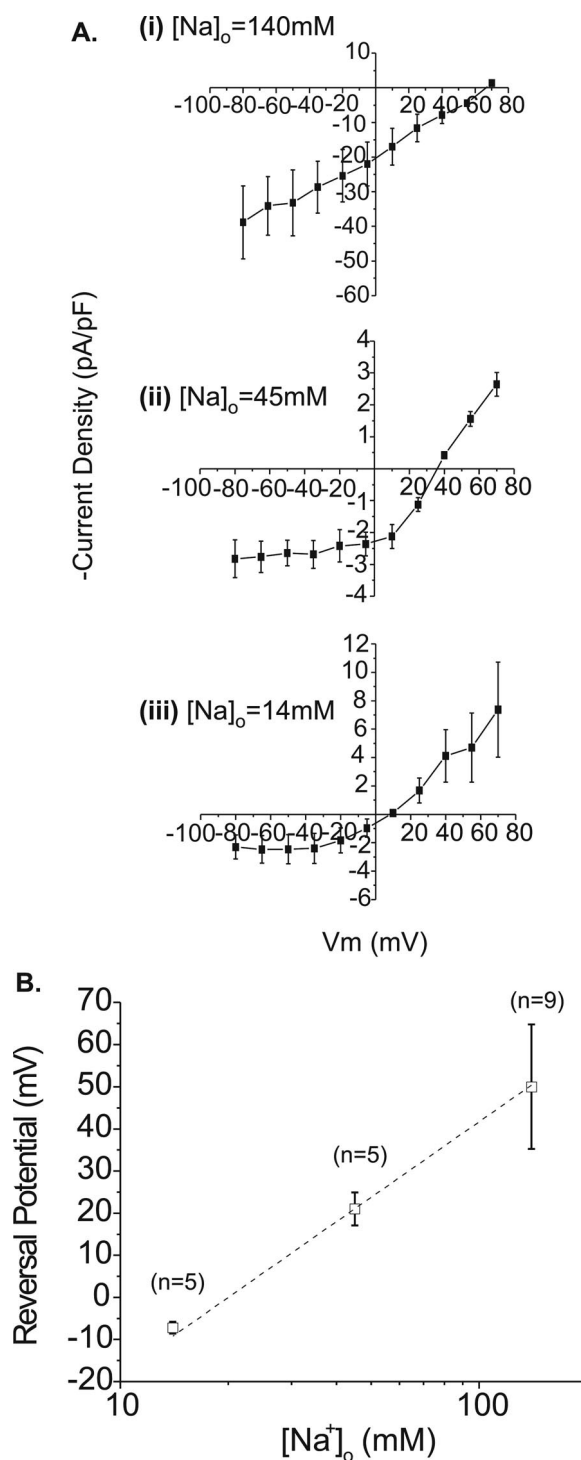


Figure 4. Varying extracellular Na^+ concentration causes a Nernstian shift in the reversal potential of the peak acid-evoked current in rat retinal ganglion cells. *Ai–Aiii*, Current–voltage relationships (normalized in terms of current density) measured in three different concentrations of extracellular Na^+ as indicated in the figure ($n = 9, 5$, and 5 for decreasing $[Na^+]_o$). *B*, Comparison of mean-measured reversal potentials adjusted for ionic activity (squares; \pm SEM) and theoretical reversal potentials for channels conducting Na^+ alone derived using the Nernst equation (dashed line).

Ca^{2+} channels after cell depolarization. Cd^{2+} does not inhibit the proton-gated current directly. Figure 5C shows voltage-clamp measurements of pH 4.5-evoked currents to be identical in the presence and absence of 100 μ M Cd^{2+} . Of the other 20 cells tested, 15 showed no response to acidification, but 5 showed a

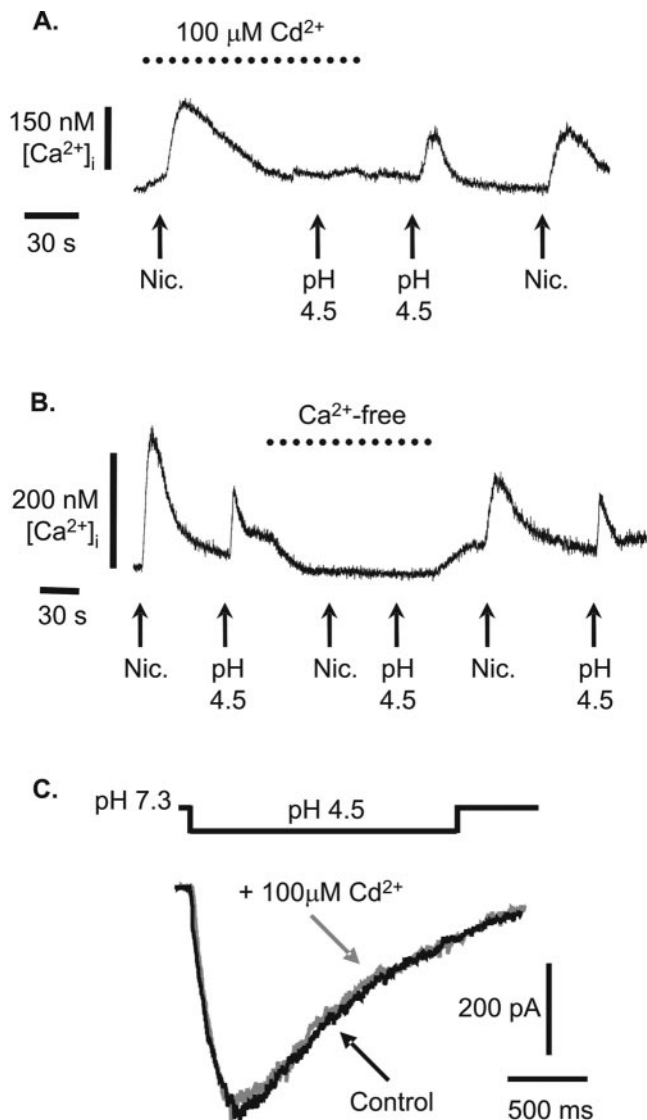


Figure 5. Intracellular Ca^{2+} changes in rat retinal ganglion cells in response to extracellular acidification. *A, B*, Cells were loaded with Indo-1/AM, and changes in the 405/488 nm emission ratio converted to changes in $[\text{Ca}^{2+}]_i$ (see Materials and Methods). In the presence and absence of either 100 μM Cd^{2+} (*A*) or extracellular Ca^{2+} (*B*), cells were challenged with 100 μM nicotine (nic.; positive control; pH 7.33) and appropriately modified extracellular solution acidified to pH 4.5. *C*, pH 4.5-evoked currents in a voltage-clamped rat retinal ganglion cell (-80 mV) are unaffected by the presence of 100 μM Cd^{2+} .

reproducible decrease from a “resting” intracellular Ca^{2+} level of 30.4 ± 5.8 nM probably reflecting the effect of a reduction in driving force on calcium influx pathways involved in intracellular store refill. Figure 5*B* demonstrates that source of the increase in Ca^{2+} seen in response to both nicotine and pH 4.5 solution is extracellular in origin. Intracellular stores are not involved, because repeating applications of nicotine and pH 4.5 solution to ganglion cells in the absence of extracellular Ca^{2+} prevents the control Ca^{2+} responses seen both before and after ($n = 7$). Moreover, during the test period in which the cell was bathed in Ca^{2+} -free solution, a clear lowering of the baseline occurred (as seen in Fig. 5*B*), providing additional evidence of a degree of Ca^{2+} influx at rest.

$I_{\text{Na}(\text{H}^+)}$ is inhibited by amiloride

ASICs are sensitive to block by the diuretic amiloride. Therefore, $I_{\text{Na}(\text{H}^+)}$ was tested for amiloride sensitivity by pre-exposing cells

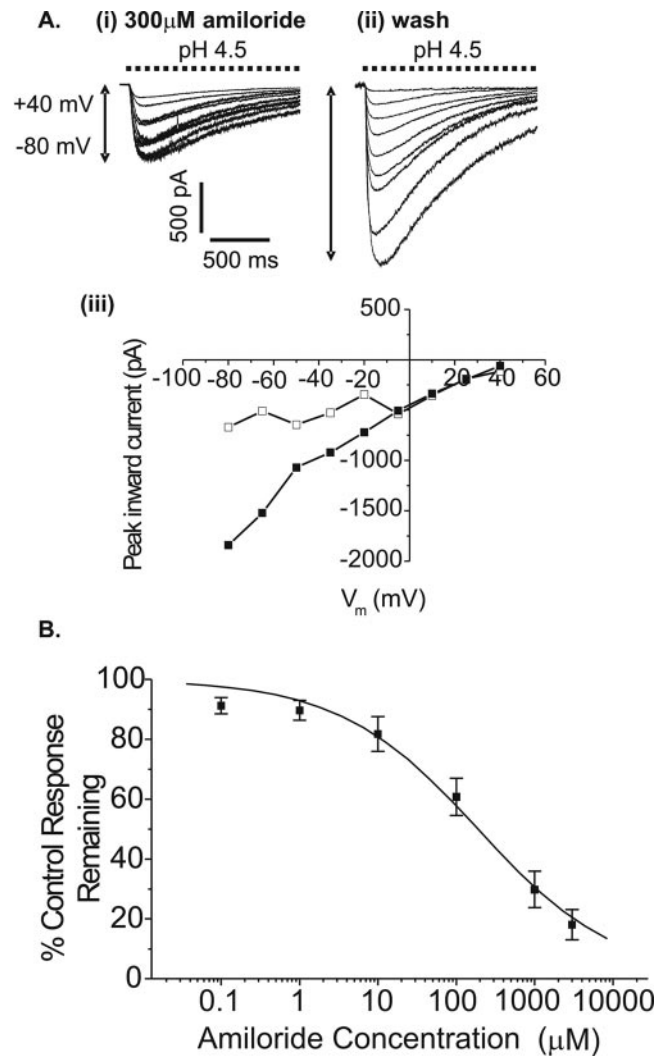


Figure 6. Effect of amiloride on the proton-gated current of rat retinal ganglion cells. *A*, pH 4.5-evoked currents recorded from a single voltage-clamped cell between -80 and $+40$ mV in 15 mV increments, in the presence (*i*) and absence (*ii*) of 300 μM amiloride. *Aiii* shows the current–voltage relationships from *Ai* (squares) and *Aii* (circles). *B*, Cells were voltage clamped at -80 mV, bathed in amiloride for 60 sec (0.1, 1, 10, 100, 1000, or 3000 μM in random order), and multiple pH 4.5-evoked currents were recorded at 60 sec intervals until steady-state block was observed. Mean peak inward currents shown above (\pm SEM; $n = 5$ –8 cells) have been normalized to amiloride-free control recorded just before every amiloride application. Sigmoidal curve parameters: IC_{50} , 188 ± 39 μM ; slope, 0.49 ± 0.05 .

for 60 sec to amiloride before applying pressure pulses of pH 4.5 solution. The addition of amiloride had no effect on the pH of the extracellular bathing solution. Two or three responses to pH 4.5 were then obtained (at 1 min intervals) to ensure that degree of block by the drug had reached equilibrium. The recordings shown in Figure 6*A* were made by subjecting a single cell to the full current–voltage protocol in the presence (*Ai*) and absence (*Aii*) of 300 μM amiloride, with the corresponding I – V relationships shown in Figure 6*Aiii*. This example indicates that amiloride block is most effective at more negative membrane potentials. For this reason, all of the data used to compile the amiloride concentration–response curve was obtained while cells were voltage clamped at -80 mV. Amiloride concentrations were tested in random order; each cell was washed between administrations to re-establish the control pH 4.5 response. A plot of mean percentage inhibition of control current by each concentration of amilo-

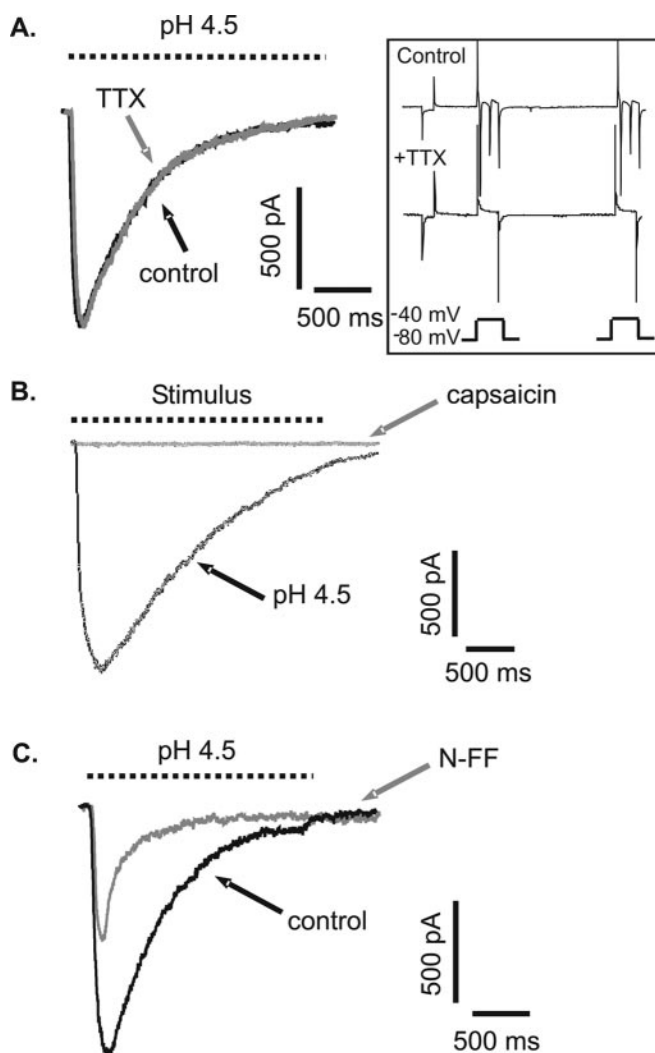


Figure 7. Modulation of retinal ganglion cell proton-gated currents by TTX, capsaicin, and neuropeptide FF. Rat retinal ganglion cells were voltage clamped at -80 mV, and acute stimuli (dashed lines) were applied by pressure pulse. *A*, pH 4.5-evoked currents were not blocked by perfusion with $0.5 \mu\text{M}$ TTX. The action of TTX was unaffected by the change in extracellular pH. Inset, Depolarization-evoked Na^+ currents were still blocked by TTX in pH 4.5 extracellular solution. Spikes in the presence of TTX are uncompensated capacitance transients (see Results for explanation). *B*, pH 4.5-evoked and $0.5 \mu\text{M}$ capsaicin-evoked currents recorded from the same cell. *C*, pH 4.5-evoked currents recorded in the absence and presence of $50 \mu\text{M}$ N-FF.

ride is shown in Figure 6*B*. This semi-log plot shows a clear concentration-dependent decrease in the size of the pH 4.5-evoked current. The data in this figure are fitted with a logistic function, the slope of which is 0.49 ± 0.05 . The IC_{50} indicated by the curve was $188 \pm 39 \mu\text{M}$.

Investigation of other potential modulators of $\text{I}_{\text{Na}(\text{H}^+)}$

TTX, which blocks the majority of voltage-gated Na^+ currents, was tested for its effectiveness against the retinal ganglion cell proton-gated current. Pressure pulses of pH 4.5 solution were applied to a cell voltage clamped at -80 mV in the absence and presence of $0.5 \mu\text{M}$ TTX. In both cases, peak current and rate of desensitization were identical ($n = 4$), as illustrated in Figure 7*A*. The effectiveness of TTX at blocking voltage-gated Na^+ currents at acidic extracellular pH was confirmed using cells cultured for several days that had begun to develop axons and were capable of firing action potentials. These cells were perfused with pH 4.5

extracellular solution for a few seconds, during which the command voltage was stepped from -80 to -40 mV. The extracellular solution also contained $100 \mu\text{M}$ Cd^{2+} to prevent voltage-gated Ca^{2+} channel activity. The inset in Figure 7*A* is a voltage step in the absence (control) and presence (+TTX) of $0.5 \mu\text{M}$ TTX in the same cell. Uncompensated capacitance transients are present at the beginning and end of both traces because of the extent of cell development. The additional spikes within the first trace are Na^+ -driven action potentials that are large enough to disrupt the voltage clamp. These are absent in the presence of TTX. Thus, the action of TTX is neither effected by extracellular acidification nor effective in blocking the proton-gated current of retinal ganglion cells.

Procaine is a lipid-soluble compound that binds to a local anesthetic site deep within the voltage-gated Na^+ channel pore. This alternative blocking action was tested on the RGC proton-gated current by applying pressure pulses of pH 4.5 solution before and after a 1–2 min incubation with 10 mM procaine (pH 7.33). Procaine did not significantly alter the peak amplitude or time constant of desensitization of the pH 4.5-evoked current ($n = 4$; data not shown).

Transient receptor potential vanilloid 1 (TRPV1) channels can also conduct depolarizing currents in response to activation by protons. In rat retinal ganglion cells, the direct application of the vanilloid receptor agonist capsaicin ($0.5 \mu\text{M}$, buffered to pH 7.33) did not evoke any depolarizing current, whereas pH 4.5 continued to be effective in evoking responses in the same cells ($n = 5$; see Fig. 7*B* for an example).

Zinc ions have been demonstrated to enhance currents conducted via ASIC2a subunit-containing channels (Baron et al., 2001, 2002). In the present study, application of ZnCl_2 (0.1 – 1 mM) to retinal ganglion cells produced a small inhibition of the acid-evoked current. At pH 4.5, the current was inhibited by $8.8 \pm 6.7\%$ in the presence of $300 \mu\text{M}$ ZnCl_2 ($n = 4$). At the less acid pH of 6.5, the inhibition was $10.3 \pm 24.1\%$ ($n = 3$).

The molluscan neuropeptide FMRFamide directly activates one nonmammalian member of the EnaC–DEG superfamily of ion channels. This peptide, together with its mammalian equivalent, N-FF, has been shown to be capable of modulating both ASIC currents and proton-gated ion currents thought to be attributable to ASICs in mammalian neurons (Askwith et al., 2000). In rat retinal ganglion cells, direct application of either peptide (3 – $30 \mu\text{M}$) did not evoke any response ($n = 6$). However, perfusing the cells with peptide (buffered to pH 7.33) and then applying pressure pulses of pH 4.5 solution revealed that both peptides could, to different degrees, modulate the proton-gated current in these cells. Surprisingly, $50 \mu\text{M}$ FMRFamide had just a small effect on rate of inactivation, increasing the time constant from 585 ± 72 msec (mean \pm SEM) to 753 ± 109 msec ($p < 0.05$; paired t test; $n = 4$) with no alteration of current amplitude. The effect of $50 \mu\text{M}$ N-FF was much more pronounced, with a marked reduction in peak current amplitude and shortening of the time constant of inactivation. Figure 7*C* shows an example of this effect. In three cells tested, the time constant decreased significantly from 532 ± 74 to 225 ± 26 msec ($p < 0.05$; paired t test).

The effect of acute exposure to acid on RGC electrical activity

RGCs are unique among retinal neurons in that they can sustain prolonged electrical activity in the form of trains of action potentials (Dowling, 1987) (Fig. 8, inset). To trigger these all-or-nothing responses, they require depolarization from resting potential in the order of 20 – 30 mV. Would the depolarization

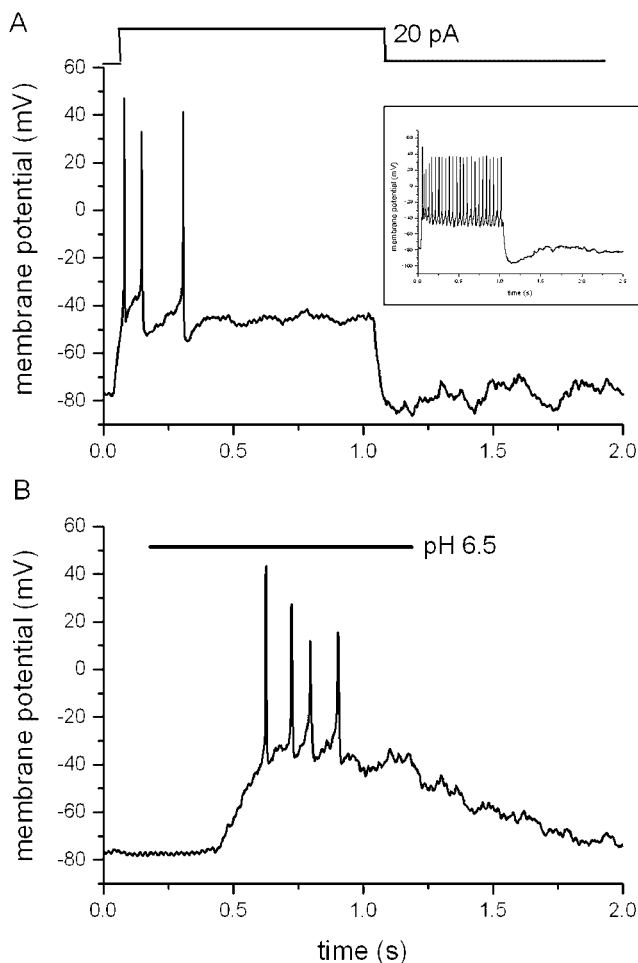


Figure 8. *A, B*, Electrical activity recorded from a current-clamped rat retinal ganglion cell in response to a 1 sec, 20 pA current injection (*A*) and pressure application of pH 6.5 for 1 sec, 8 psi (*B*). Resting $V_{m,r}$ = -78 mV. Inset shows strong repetitive firing in response to a 1 sec, 50 pA current injection.

caused by transient extracellular acidification be sufficient to trigger action potential generation? With mean cell input resistances of $1.54 \pm 0.7 \text{ G}\Omega$ ($n = 50$), just 16.2 pA would be required to elicit a change in membrane potential of 25 mV. Because currents of this magnitude were generated by pH 6.5, pressure pulses of pH 6.5 solution were applied to cells held in current-clamp mode at their resting potential. Figure 8 shows a single RGC from which electrical responses to both current injection (*A*) and acute acidification (*B*) were recorded (V_{rest} in this example was -78 mV). Current injection of 20 pA was the minimum required for this particular cell to reach action potential threshold (estimated at -45 mV from Fig. 8*A*). Pressure-pulse application pH 6.5, demonstrated above as the threshold pH for current activation in RGCs, evoked similar short trains of action potentials ($n = 3$). However, at the more acid pH of 6.0, just one cell produced an action potential and, in an additional 17 cells, only sustained depolarization beyond action potential threshold was seen.

Discussion

This is the first description of a proton-gated current in mammalian retinal neurons. Recently, Brockway et al. (2002) detected ASIC1, 2, 3, and 4 mRNA in rabbit retina and demonstrated the presence of an amiloride-sensitive current in retinal glial (Müller) cells. In mouse retina, ASIC3 mRNA has also been identified

(Maubaret et al., 2002). Consistent with these findings, the rat retina as a whole also appears to contain most of the ASIC subunits cloned to date, with ASICs 1a and 2a particularly abundant. The combined electrophysiological and RT-PCR data presented here suggest that ASIC the mRNA detected encodes proteins that form functional ion channels in the retina. No attempt has been made in this study to localize subunit expression within the laminar organization of retinal neurons, although other subunits from the closely related EnaC–DEG family have been detected previously in the ganglion cell layer using immunocytochemistry and *in situ* hybridization (Matsuo, 1998; Mirshahi et al., 1999; Golestaneh et al., 2000).

$I_{\text{Na(H+)}}$ in rat retinal ganglion cells

$I_{\text{Na(H+)}}$ shares most of the characteristics of currents recorded from cells transfected with ASIC proteins. When stimulated by the fast application of protons under physiological recording conditions and at resting membrane voltages, RGCs exhibit a rapidly activating inward current which, from Nernstian shifts in reversal potential with E_{Na} , is carried by Na^+ ions. RGC proton-gated channels do not appear to be Ca^{2+} permeant, nor do they show any voltage dependence of activation. During prolonged applications of acid, the current desensitizes completely, the time constant of which (in the region of 600 msec) shows no clear dependence on membrane potential or pH. These features also relate to currents conducted via channels containing ASICs 1a, 1b, or 2a, although RT-PCR results showed ASIC1b is not present in the retina. The absence of a steady-state current in the continued presence of acid and the Na^+ selectivity of $I_{\text{Na(H+)}}$ suggests that ASIC3, or the modulatory subunit 2b, does not contribute to this current. $I_{\text{Na(H+)}}$ is reversibly inhibited by amiloride but, in contrast to other ASIC currents, the IC_{50} of 188 μM appears relatively large. This probably reflects the use of stronger acid (pH 4.5 here; approximately pH 6.0 elsewhere) in generating the amiloride concentration–inhibition curve, as observed by Sutherland et al. (2001). $I_{\text{Na(H+)}}$ activation occurs as the extracellular pH falls below pH 6.5 (300 nM $[\text{H}^+]$), similar to the activation of homomeric ASIC 1a channels (Waldmann et al., 1997). In contrast, half-maximal and maximal activation occurs at much more acidic levels, closer to those of ASIC2a (Lingueglia et al., 1997). Cotransfection of rat ASIC 1a and 2a produces channels with these activation characteristics. Furthermore, a high degree of colocalization of these subunits exists within brain neurons (Basilana et al., 1997), and strong evidence of both subunits was found here in the retina. However, the lack of enhancement of $I_{\text{Na(H+)}}$ by ZnCl_2 would suggest that the channels do not contain ASIC2a, because it has been reported that Zn^{2+} enhancement is diagnostic of ASIC2a-containing channels (Baron et al., 2001, 2002). In the absence of electrophysiological data from heteromultimers containing the “silent” subunit ASIC 4, these data suggest that the proton-gated current of rat RGCs is conducted via a heteromultimeric channel containing ASIC1a and possibly ASIC4. Other as yet unidentified subunits may also contribute.

$I_{\text{Na(H+)}}$ also shows many similarities with native proton-gated currents recorded from other regions of the mammalian brain. All require rapid (msec) acidification to activate, all are insensitive to block by conventional voltage-gated Na^+ channel antagonists (demonstrated here with TTX and procaine), and their rapid recovery from desensitization plus voltage insensitivity distinguishes them from TRPV1 receptor activity. In terms of tissue-specific differences, the sensitivity of the retinal ganglion cell current to small changes in extracellular pH is reduced, which is

perhaps predictable for a tissue with an enhanced level of metabolic activity.

FMRFamide, which activates the nonmammalian peptide-gated relatives of ASICs, and the structurally similar mammalian peptide N-FF are known to significantly potentiate certain ASIC currents (Askwith et al., 2000; Catarsi et al., 2001; Allen and Attwell, 2002). These effects have so far only been observed in ASIC1 or ASIC3 homomers and ASIC2a and 3 heteromeric channels. Neither peptide potentiated $I_{\text{Na(H+)}}$, but considering that the electrophysiological and pharmacological characteristics of the current preclude ASIC2a and 3 involvement, this result is not surprising. What was surprising, however, was that N-FF significantly decreased current magnitude and shortened the time constant of desensitization. Whether N-FF itself is endogenous to the retina has yet to be established, but mRNAs encoding closely related RFamide-related peptides have recently been found in very high levels in the eyes of rats as well as the human retina (Hinuma et al., 2000), which may provide local modulation of the function of ASICs in the visual system.

Physiological role

From the current-clamp recordings shown in Figure 8, rapid but weak extracellular acidification appears to evoke the normal pattern of electrical activity associated with RGCs. However, at more acidic levels (more than pH 6.5), the effect is to depolarize the cell evoking none or a single action potential (presumably because of the “shunting effect” of opening a large number of channels or the inactivation of sodium channels). Protons therefore provide a way of modulating the excitability of these cells. The ability to detect extracellular acidification is an understandable characteristic of cells involved in nociception (e.g., DRGs) and taste. Yet, in the retina (and the CNS in general), extracellular pH is tightly regulated, and even under strong light or electrical stimulation pH fluxes do not exceed 0.1 pH unit (Borgula et al., 1989; Yamamoto et al., 1992). The largest activity-induced fluxes (up to 0.3 pH units) have been recorded in the mammalian optic nerve (Davis et al., 1987). With resting retinal pH levels within the range of pH 7.2–7.4 (Padnick-Silver and Linsenmeier, 2002), the most extreme acidification might result in the lowering of retinal pH to 6.9, which would be insufficient to activate $I_{\text{Na(H+)}}$. If this current does contribute to gross retinal physiology, it may require modulation by some other locally released factor such as a neuropeptide, or even activation by a stimulus other than protons. On the basis of their observations of ASIC3, ASIC1a, and native neuronal acid-evoked currents, Immke and McCleskey (2003) recently proposed that rather than directly activating the current, protons open ASIC channels by catalyzing the relief of channel block by calcium. The observation that a reduction in extracellular calcium enables ASICs to activate at less acidic pH levels suggests that local calcium homeostasis may play a significant role in the control of these channels (Korkushco et al., 1983; Babini et al., 2002).

Alternatively, local pH levels within synaptic clefts may fluctuate over a wider dynamic range (Krishtal, 2003). In mammalian cone photoreceptors, it has been suggested that release of vesicular protons can modulate presynaptic calcium currents and ultimately neurotransmitter release (DeVries, 2001). Additional evidence for the role of transient acidification and ASIC function in synaptic transmission comes from the observations that ASIC knock-out mice display altered synaptic potentials in the hippocampus (Wemmie et al., 2002). Until additional studies in the retina and on the visual system of ASIC knock-out mice are per-

formed, any physiological role of $I_{\text{Na(H+)}}$ in RGCs remains unclear.

Pathophysiology

Although physiological changes in pH may be small, there is evidence that changes resulting from ischemia may be much larger. Indeed, in the brain, ASIC expression is induced during ischemia (Johnson et al., 2001), and ASIC channel currents are modulated by substances released during ischemic episodes (Allen and Attwell, 2002). Retinal ischemia and other pathologies such as glaucoma also involve a decrease in extracellular pH and the selective loss of RGCs (Ikeda et al., 1992; Lu et al., 2001). If ASICs are part of a mechanism whereby the pH flux contributes to the death of these cells, they present a worthwhile target for therapeutic investigation.

Note added in proof. While this work was in proof, an article showing that Zn^{2+} inhibits only ASIC1a currents was published (Chu et al., 2003), supporting our case that the ASIC1a subunit is the most likely candidate mediating $I_{\text{Na(H+)}}$ in RGCs.

References

- Allen NJ, Attwell D (2002) Modulation of ASIC channels in rat cerebellar purkinje neurons by ischaemia-related signals. *J Physiol (Lond)* 543:521–529.
- Askwith CC, Cheng C, Ikuma M, Benson C, Price MP, Welsh MJ (2000) Neuropeptide FF and FMRFamide potentiate acid-evoked currents from sensory neurons and proton-gated DEG/ENaC channels. *Neuron* 26:133–141.
- Babini E, Paukert M, Geisler HS, Grunder S (2002) Alternative splicing and interaction with di- and polyvalent cations control the dynamic range of acid-sensing ion channel (ASIC) 1. *J Biol Chem* 276:41597–41603.
- Baron A, Schaefer L, Lingueglia E, Champigny G, Lazdunski M (2001) Zn^{2+} and H^{+} are coactivators of acid-sensing ion channels. *J Biol Chem* 276:35361–35367.
- Baron A, Waldmann R, Lazdunski M (2002) ASIC-like, proton activated currents in rat hippocampal neurons. *J Physiol (Lond)* 539:485–494.
- Bassilana F, Champigny G, Waldmann R, de Weille JR, Heurteaux C, Lazdunski M (1997) The acid-sensitive ionic channel subunit ASIC and the mammalian degenerin MDEG form a heteromultimeric H^{+} -gated Na^{+} channel with novel properties. *J Biol Chem* 272:28818–28822.
- Bassler E-L, Ngo-Anh TJ, Geisler H-S, Ruppersberg JP, Grunder S (2001) Molecular and functional characterisation of acid-sensing ion channel (ASIC) 1b. *J Biol Chem* 276:33782–33787.
- Baumann TK, Burchiel KJ, Ingram SL, Martenson ME (1996) Responses of adult human dorsal root ganglion neurons in culture to capsaicin and low pH. *Pain* 65:31–38.
- Benson CJ, Sutherland SP (2001) Toward an understanding of the molecules that sense myocardial ischemia. *Ann NY Acad Sci USA* 940:96–109.
- Borgula GA, Steinberg RH, Karwowski CJ (1989) Light-evoked changes in extracellular pH in frog retina. *Vision Res* 29:1069–1077.
- Brockway LM, Zhou ZH, Bubien JK, Jovov B, Benos DJ, Keyser KT (2002) Rabbit retinal neurons and glia express a variety of ENaC/DEG subunits. *Am J Physiol* 283:C126–C134.
- Catarsi S, Babinski K, Séguéla P (2001) Selective modulation of heteromeric ASIC proton-gated channels by neuropeptide FF. *Neuropharmacology* 41:592–600.
- Chesler M (1990) The regulation and modulation of pH in the nervous system. *Prog Neurobiol* 34:401–427.
- Chomczynski P, Sacchi N (1987) Single-step method of RNA isolation by acid guanidinium thiocyanate phenol chloroform extraction. *Anal Biochem* 162:156–159.
- Chu XP, Zhu XM, Wemmie JA, Price MP, Saugstad JA, Simon RP, Welsh MJ, Xiong ZG (2003) Subunit-dependent high affinity zinc inhibition of acid-sensing ion channels. *Soc Neurosci Abstr* 29:308.7.
- Davis PK, Carlini WG, Ransom BR, Black JA, Waxman SG (1987) Carbonic-anhydrase activity develops postnatally in the rat optic-nerve. *Dev Brain Res* 31:291–298.
- de la Rosa DA, Canessa CM, Fyfe GK, Zhang P (2000) Structure and regulation of amiloride-sensitive sodium channels. *Ann Rev Physiol* 62:573–594.

- DeVries SH (2001) Exocytosed protons feedback to suppress the Ca^{2+} current in mammalian cone photoreceptors. *Neuron* 32:1107–1117.
- de Weille JR, Bassilana FR, Lazdunski M, Waldmann R (1998) Identification, functional expression and chromosomal localisation of a sustained human proton-gated cation channel. *FEBS Lett* 433:257–260.
- Dowling JE (1987) The retina: an approachable part of the brain, pp 82–83. Belknap: Harvard UP.
- Gilbertson TA, Roper SD, Kinnamon SC (1993) Proton currents through amiloride-sensitive Na^{+} channels in isolated hamster taste cells—enhancement by vasopressin and cAMP. *Neuron* 10:931–942.
- Golestaneh N, Nicolas C, Picaud S, Ferrari P, Mirshahi M (2000) The epithelial sodium channel (ENaC) in rodent retina, ontogeny and molecular identity. *Curr Eye Res* 21:703–709.
- Hayat S, Wigley CB, Robbins J (2003) Intracellular calcium handling in rat olfactory ensheathing cells and its role in axonal regeneration. *Mol Cell Neurosci* 22:259–270.
- Hinuma S, Shintani Y, Fukusumi S, Lijima N, Matsumoto Y, Hosoya M, Fujii R, Watanabe T, Kikuchi K, Terao Y, Yano T, Yamamoto T, Kawamata Y, Habata Y, Asada M, Kitada C, Kurokawa T, Onda H, Nishimura O, Tanaka M, Ibata Y, Fujino M (2000) New neuropeptides containing carboxy-terminal RFamide and their receptor in mammals. *Nat Cell Biol* 2:703–708.
- Ikeda H, Hankins MW, Asai T, Dawes EA (1992) Electrophysiological properties of neurons following mild and acute retinal ischemia. *Exp Eye Res* 55:435–442.
- Immke DC, McCleskey EW (2003) Protons open acid-sensing ion channels by catalyzing relief of Ca^{2+} blockade. *Neuron* 37:75–84.
- Johnson MB, Jin K, Minami M, Chen D, Simon RP (2001) Global ischemia induces expression of acid-sensing ion channel 2a in rat brain. *J Cereb Blood Flow Metab* 21:734–740.
- Krishtal O (2003) The ASICs: signaling molecules? modulators? *Trends Neurosci* 26:477–483.
- Korkushko AO, Krishtal OA, Chernevskaia NI (1983) Steady-state characteristics of the proton receptor in the somatic membrane of rat sensory neurons. *Neirofiziologia* 15:632–638.
- Kovalchuk YN, Krishtal OA, Nowycky MC (1990) The proton-activated inward current of rat sensory neurons includes a calcium component. *Neurosci Lett* 115:237–242.
- Li YX, Schaffner AE, Li HR, Nelson R, Barker JL (1997) Proton-induced cation current in embryonic rat spinal cord neurons changes ion dependency over time *in vitro*. *Dev Brain Res* 102:261–266.
- Lilley SJ (2001) The discovery and characterisation of a proton-gated sodium current in rat retinal ganglion cells. PhD thesis, University of London.
- Lilley S, Robbins J (2001) Characterisation of a novel proton-gated sodium current in rat retinal ganglion cells. *J Physiol (Lond)* 531:83P–84P.
- Lingueglia E, deWeille JR, Bassilana F, Heurteaux C, Sakai H, Waldmann R, Lazdunski M (1997) A modulatory subunit of acid sensing ion channels in brain and dorsal root ganglion cells. *J Biol Chem* 272:29778–29783.
- Lu DW, Chang CJ, Wu JN (2001) The changes of vitreous pH values in an acute glaucoma rabbit model. *J Occ Pharmacol Ther* 17:343–350.
- Matsuo T (1998) Expression of amiloride-sensitive sodium channel in rat eye. *Acta Medica Okayama* 52:279–283.
- Maubaret C, Delettre C, Sola S, Hamel CP (2002) Identification of preferentially expressed mRNAs in retina and cochlea. *DNA Cell Biol* 21:781–791.
- Mirshahi M, Nicolas C, Mirshahi S, Golestaneh N, d'Hermies F, Agarwal MK (1999) Immunochemical analysis of the sodium channel in rodent and human eye. *Exp Eye Res* 69:21–32.
- Padnick-Silver L, Linsenmeier RA (2002) Quantification of *in vivo* anaerobic metabolism in the normal cat retina through intraretinal pH measurements. *Vis Neurosci* 19:793–806.
- Price MP, Lewin GR, McIlwrath SL, Cheng C, Xie JH, Heppenstall PA, Stucky CL, Mannsfeldt AG, Brennan TJ, Drummond HA, Qiao J, Benson CJ, Tarr DE, Hrstka RF, Yang BL, Williamson RA, Welsh MJ (2000) The mammalian sodium channel BNC1 is required for normal touch sensation. *Nature* 407:1007–1011.
- Reeh PW, Steen KH (1996) Tissue acidosis in nociception and pain. *Prog Brain Res* 113:143–151.
- Robbins J, Reynolds AM, Treseder S, Davies R (2003) Enhancement of low-voltage-activated calcium currents by group II metabotropic glutamate receptors in rat retinal ganglion cells. *Mol Cell Neurosci* 23:341–350.
- Robinson RA, Stokes RH (1959) Electrolyte solutions, Sec 5, p 4. London: Butterworth.
- Sutherland SP, Benson CJ, Adelman JP, McCleskey EW (2001) Acid-sensing ion channel 3 matches the acid-gated current in cardiac ischemia-sensing neurons. *Proc Natl Acad Sci USA* 98:711–716.
- Ueno S, Nakaye T, Akaike N (1992) Proton-induced sodium current in freshly dissociated hypothalamic neurons of the rat. *J Physiol (Lond)* 447:309–327.
- Varming T (1999) Proton-gated ion channels in cultured mouse cortical neurons. *Neuropharmacol* 38:1875–1881.
- Waldmann R, Champigny G, Bassilana F, Heurteaux C, Lazdunski M (1997) A proton-gated cation channel involved in acid-sensing. *Nature* 386:173–177.
- Wemmie JA, Chen J, Askwith CC, Hruska-Hageman AM, Price MP, Nolan BC, Yoder PG, Lamani E, Hoshi, Freeman JH, Welsh MJ (2002) The acid-activated ion channel ASIC contributes to synaptic plasticity, learning and memory. *Neuron* 34:463–477.
- Yamamoto F, Borgula GA, Steinberg RH (1992) Effects of light and darkness on pH outside rod photoreceptors in the cat retina. *Exp Eye Res* 54:685–697.